Appl Phys B (2008) 93: 79–89
DOI 10.1007/s00340-008-3213-1

Applied Physics B
Lasers and Optics

Interface-induced dephasing of Mie plasmon polaritons

U. Kreibig

Received: 2 July 2008 / Revised version: 14 August 2008 / Published online: 12 September 2008

Abstract Surface and, in particular, interface effects influence all physical and chemical properties of nanostructured matter. Mie surface plasmon polaritons (MPPs) in metallic nanoparticles are excellent and sensitive sensors for optical investigation of these effects of realistic particles since their lifetimes due to dephasing (decoherence) effects and their resonance energies drastically depend upon the chemistry and topology of their surfaces/interfaces. A survey is given over some results of our own long term research on MPPs which started, in fact, as early as 1969. Theoretical models and experiments concerning the A parameter, the δn parameter, MPP phase decoherence and static and dynamic interface charge transfer effects ("chemical interface damping") are briefly summarized. The effect of radiation damping is disregarded throughout: we assume the particle sizes to be small enough to justify this simplification, which makes it easier to draw conclusions from the MPPs on nanomaterial properties. Obviously, there is a wide field for future research concerning particle interfaces on the basis of Mie's theory. On the other hand, all of these effects have to be incorporated into Mie's theory to obtain a "modern" version which is reliable on a quantitative level to describe experimental data.

PACS 61.46.Df · 71.45.Gm · 72.10.Gm · 73.20.-r · 73.22.-b · 73.40.Ns · 78.67.-n

U. Kreibig (✉)
Physikalisches Institut 1A der RWTH Aachen, Aachen, Germany
e-mail: kreibig@physik.rwth-aachen.de

1 Introduction

Metallic nanoparticles of (almost) spherical shape are fundamental objects in modern nanoscience research fields like nano-optics, nanophotonics and nanoplasmonics, only to cite a few concerning optics. The reason is the existence of the unique Mie resonances. In the frame of electrodynamics, their origin is open, and they are excited, irrespective of their physical origin, if special numerical conditions of the Maxwell boundary conditions, i.e. special data sets of the dielectric function of the particle material (DF), the dielectric constant $\varepsilon_{\text{Medium}}$ of the surrounding materials, the wavelength λ and the particle size R, are fulfilled.

Since DFs are external material quantities in the frame of electrodynamics, their origin in the spectral range of resonance frequencies can only be identified with help of solid state physics. We, therefrom, can learn whether the resonance is due to single electron band structure transitions or to collective, coherent excitations of the plasma of conduction electrons. In the latter case they are really Mie plasmon polaritons (MPPs). Metal particles often exhibit several Mie resonances. To give an example, in Y nanos we find three, differently damped ones. Only good "free-electron" metals like the noble and alkali metals exclusively exhibit plasmonic resonances.

Metal particles act as receiving and at same time as emitting antennas for incident light, which, under the special conditions above, can induce forced excitations of plasma oscillations or, in the quantum picture, of surface plasmons. These are, in fact, polaritons, since they are coupled, via incident and scattered light, to the external electromagnetic field. The, now 100 years old, Mie theory [1], being the formal analog to Fresnel's formulae, for spherical sample symmetry, describes the linear optical response of the particles, including collective excitations, by expansion of the

Table 1 Reality beyond Mie's theory. The table shows effects, missing or unrealistically considered in the original ("classical") Mie theory. $\surd$ indicates that supplementing models exist. References: see [3]

(A) Electrodynamic theory		(B) Material properties	
(1) Incident wave not plane (e.g. focused laser beam)	($\surd$)	(9) Dielectric function of the particle material differs from bulk DF due to size effects: $\varepsilon = \varepsilon(\omega, R)$	$\surd$
(2) The step-like Maxwell boundary conditions do not hold	($\surd$)		
(3) Particles electrically charged due to chemical potential	$\surd$	(10) Dielectric function of the particle material is not locally homogeneous due to surface properties: $\varepsilon = \varepsilon(\omega, r)$	
(4) Particle shapes not spherical	($\surd$)		
(5) Particle sizes in many-particle systems not uniform	$\surd$	(11) Changes due to static and dynamic charge transfer	$\surd$
(6) Heterogeneous particle structures: core/shell, multigrain	$\surd$	(12) Dielectric function of particle material is non-linear	
(7) Dense packing in many-particle systems: electrodynamic particle–particle coupling	$\surd$	(13) Dielectric function of the matrix $\varepsilon_{\text{Medium}}$ varies with frequency	$\surd$
		(14) Dielectric function of the matrix is complex (absorbing matrix)	$\surd$
(8) Tensorial dielectric function		(15) Dielectric function of the matrix material is non-linear	$\surd$

involved fields into series of orthogonal multipole modes, the Mie plasmon polariton modes. However, it lasted until 1970 to identify experimentally special Mie resonances in metal particles as being MPPs [2].

The theory of Mie is an exact solution of linear electrodynamics, however with assumptions which, in part, are far away from reality in the nanoscale region. So, comparing Mie's *original* theory with realistic nanoparticle experiments often ends with frustrating discrepancies. As a consequence, many more or less successful attempts have been performed to introduce modifications, extensions and corrections into Mie's theory [3]. The thus resulting *modern* Mie theory has become a powerful tool in nano-optics and surface science which is reliable also to a quantitative degree. (Problems arise, however, from the quality of part of the supplementing models.)

Table 1 shows a survey over identified deficits of the *original* ("classical") theory which were, in part, corrected to enable a closer approach to reality. For details, for a lot of other effects and for references we refer the reader to [3].

In the following we shall pick out one of these topics beyond Mie's original theory and demonstrate in detail the realistic influences of surrounding media or of substrates on the linear optical extinction properties of a metallic nanoparticle. We will, however, not treat here related topics like interpretations of chemical surface/interface reactions [5] or the recent result that the single-electron interband transitions in silver particles also exhibit a dependence on embedding media [6]; instead, we only point to the according literature.

This paper is not intended to give a topical review; instead, it is a report on own research. Hence, the reference list is incomplete and mainly includes papers which are directly related to this research. To give examples of extended reviews about electron dynamics in metallic nanos which include numerous references, we refer the reader to Aeschlimann [7], to Hubenthal [8] and to Pinchuk et al. [9].

2 Surfaces and interfaces of nanoparticles

Mostly, particles in nature and technology do not have free, uncontaminated surfaces; instead, they are part of complex systems, consisting of the particles, the solid or liquid surroundings, both with inhomogeneous optical properties, and the inhomogeneous interface region between them. This region consists of a three-dimensional layer of several nm thickness, and usually contains special electronic interface states, which, in general, can strongly differ from both the electronic states in the separate particle and in the surrounding material.

The main advantage of Mie's theory compared with quantum theoretical calculations is that it is not limited to jellium or similar rough models of the particle material. Instead, the frequency-dependent, in general, complex dielectric function (DF) of the realistic particle material, $\varepsilon_1(\omega) + i\varepsilon_2(\omega)$, and the real dielectric constant $\varepsilon_{\text{Medium}}$ of the surrounding material (assumed by Mie to be dielectric, i.e. non-absorbing) are explicitly included in the electrodynamic formulae. Hence, we can numerically distinguish between the extinction characteristics of Ag and of Y particles, to give an example. However, the way in which Mie did this rather reduces this advantage.

We know today that Mie's assumption of "sharp" Maxwellian boundary conditions does not hold on the nanoscale. Instead of a step function, there are smooth transitions of the polarizability from the metal particle to the interlayer and to the surroundings [3]. In contrast, the step function, used by Mie, enforces that his formulae are based upon only *one* homogeneous value of the DF in the whole particle and *one* value of the frequency-independent dielectric constant of the matrix material. Thus, all realistic surface and interlayer properties are ignored. The importance of these nano-effects increases towards smaller particles, thus rendering the DF size dependent. The effects on calculated Mie spectra are drastic in particles of good "free-electron" metals [3];

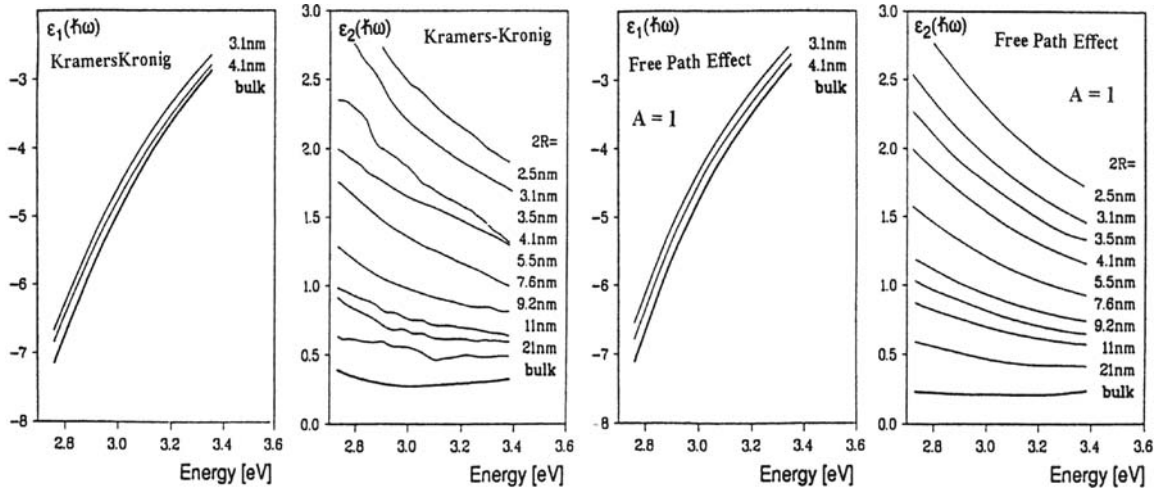

Fig. 1 Spectra of the dielectric function (DF) of Ag particles of various sizes, embedded in a glass matrix [3]. Two graphs at *left*: obtained from measured MPP spectra by combining Mie's theory with a Kramers–Kronig analysis. Two graphs at *right*: obtained by a model calculation including dephasing at the metal/glass interface

they remain small in many other materials. So, the selection of proper DF spectra is a crucial matter.

The worst case is if, in succession to Mie himself, the DFs are chosen to be those measured from bulk, possibly even monocrystalline, material. In good "free-electron" metals, the DF converges towards the bulk DF only for particle sizes larger than some 10 nm.

By the way, the application of this fictitious homogeneous DF is one of the reasons why the process of particle deposition on a substrate is, even 100 years after the appearance of Mie's theory, not yet sufficiently well understood.

Today, methods have been developed to include nanosize and interface effects into the DF of bulk material by introducing correction terms (e.g. [3]). Hence, we obtain *one* fictitious homogeneous DF for the real particle material, as necessary for Mie's formulae, but properly corrected for nano-effects. In fact, it is a volume average, even including the surface/interface region. (A proper way to treat these problems would be to replace the, generally, macroscopically defined DF by locally varying polarizabilities. This has, to our knowledge, not yet been attempted in analytical form. It should be possible by applying numerical evaluation methods.)

Figure 1 presents spectra of the size- and interface-corrected, homogeneous DF for Ag particles of various sizes, embedded in glass [3]. They were obtained by "inverse" application of Mie's theory. This means that measured absorption spectra were introduced into Mie's formulae and the corresponding DF values were then numerically fitted, with assistance of a Kramers–Kronig analysis. So, the presented DF is the one, which, introduced in Mie's theory, would yield absorption spectra quantitatively corresponding with the experimental input spectra.

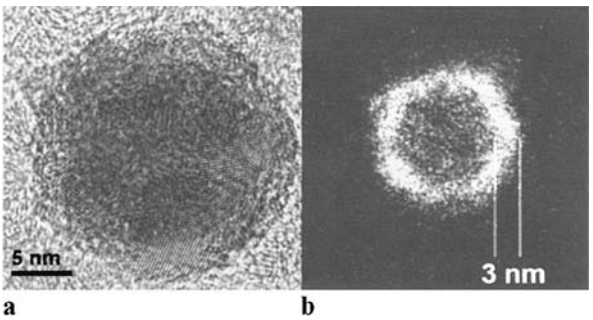

Fig. 2 HRTEM and EFTEM micrograph of a Co/CoO_x, $x \leq 2$, core/shell particle [10]

The two graphs at left show the results of this evaluation of measured optical absorption spectra; the two at right are the results of a size-effect model [3]. In particular, $\varepsilon_2(\omega)$, which contributes to the plasmon damping, changes with varying silver particle size by more than a factor of 10. These results, by the way, also demonstrate that the "inverse" application of Mie's theory is successful and can open the door to determine nanostructure effects in the optical material properties and to manipulate them.

Surrounding matrices or substrates are inevitable for most inorganic nanoparticle applications because nanos are usually thermodynamically unstable due to their immense surface energies (5 keV in a single free 10-nm Ag particle). These stabilizing surroundings can prevent aggregation an coalescence of neighboring particles. Alternative stabilizings are due to the formation of surface layers by adsorbates, by oxide shells [10] (Fig. 2) and so on, with relative "surface coverage areas", i.e. the part of the surface with *direct* contact to foreign material at atomic distances, smaller or larger than 1.

It appears obvious that these interface regions have strong influences on MPPs, since the latter are essentially surface/interface-driven excitations and hence extremely sensitive against any change of structural, chemical or electronic interface properties. So, the MPPs offer themselves as highly sensitive tools for future research on realistic surfaces and interfaces on the nanoscale. Already nowadays they are applied for a broad variety of chemical and biological sensor applications.

In the following a special model will be presented to illustrate electronic processes occurring in the interface and their implications in the excitation of MPPs.

We shall restrict ourselves to silver nanoparticles since they exhibit the largest resonance enhancement of the inner field and, thus, the most pronounced Mie resonances in the extinction spectra, of all materials which we know of. In particular, the MPPs surpass those of Au nanos, where the (size-dependent) interband transition edge, situated at 2.45 eV (3.8 eV in Ag), superimposes partly the Mie resonances, thus opening an additional excitation decay channel. The particle sizes are chosen very small (between 2 and 15 nm), so radiation damping [3, 11], retardation effects and the excitation of higher multipolar order MPPs beyond the dipolar one can be neglected. This simplification is justified by our aim to describe special material properties on the nanoscale.

3 Interface effects upon the MPPs

It has been proven experimentally [5] that the existence of an interlayer influences MPPs to extents which were often underestimated before. Both the peak position and its width (i.e. the relaxation) are concerned. A small part of the observed peak shifts and the whole increase of observed resonance widths cannot be explained in the frame of Mie's original theory from the reasons stated above, and have to be modeled separately.

In the following we introduce the model of "static" and of "dynamic" charge transfer [5], earlier [12] also called "chemical interface damping".

Inside the nano, the "collisions" of the free electrons contribute to the MPP damping either by the various processes known from bulk Drude material, or by additional interactions with the surface, leading to a limitation of the electron mean free path [3]. (Alternatively, the latter process can also be interpreted as a "quantum size effect" [3].) At the free surface, these interactions presuppose mainly elastic reflections. This changes drastically if the free surface is replaced by an interface region, because the surface colliding electrons can now occupy empty interface states, if present [5]. So, the MPP relaxation processes may drastically depend on the structure and the chemical composition of the surrounding medium.

The MPP bandwidth Γ for Ag particles (derived in the "quasistatic dipole approximation", i.e. by neglecting radiation damping [3, 4], retardation and higher MPP mode contributions) is given by [5]

$$\Gamma(A,R) \approx \Gamma_0 + \Delta\Gamma = \Gamma_0 + \left(2\omega_p^2/\omega^3\right) \times \left[(d\varepsilon_1/d\omega)^2 + (d\varepsilon_2/d\omega)^2\right]^{-1/2} (v_{\mathrm{Fermi}} \cdot A/R). \quad (1)$$

with ω_p the Drude plasma frequency and v_{Fermi} the Fermi velocity. The proper DF includes size and surface/interface dependences. $\Delta\Gamma$ of (1) consists of a dissipation and a dispersion contribution [3]:

$$\Delta\Gamma \approx (\text{dissipation term})/(\text{dispersion term}). \quad (2)$$

Γ_0 is the bandwidth following from "classical" Mie theory. The effect of dispersion on Γ in (2) is that it determines how rapidly the absorption decreases from the peak maximum when the frequency is *detuned* from the Mie resonance frequency.

The damping quantity ε_2 contains a hierarchy of different electronic relaxation processes [7], which are assumed to be statistically "memory destroying". The decay of the MPP, i.e. Γ, is dominated by the fastest among them, and this is a phase relaxation (*dephasing* or *phase decoherence*) of the collective excitation with a phase decay relaxation time τ_{Phase}.

This quantity has been investigated by various experimental methods [7], like optical methods (Hövel et al. [12], Klar et al. [11]), hole burning (Stietz et al. [13], Ziegler et al. [14], Hendrich et al. [15]), pump–probe SHG (Lamprecht et al. [16], Rubahn and co-workers [17]) and THG (Lamprecht et al. [18]).

An extended research report was presented also by Hubenthal [8] in his habilitation thesis.

When $\varepsilon_{\mathrm{Medium}}$ is changed, the Maxwell boundaries induce the "dielectric shift" of the MPP peak position, since the restoring force of the surface polarization is altered [3]. This interface influence is contained in Mie's theory. To give a numerical example: varying $\varepsilon_{\mathrm{Medium}}$ from 1 to 6 causes the peak of Ag particles to red shift over the whole visible region. In the special case of Ag, the dispersion in (4) towards the blue (see e.g. Fig. 1) decreases by contributions of the UV interband transition edge to ε_1 and, hence, Γ is markedly narrowed when ε medium is enlarged. Thus, Γ is not a proper measure of the MPP relaxation lifetime for realistic materials like Ag. (Only in the Drude case the width does not change with peak frequency, and Γ is identical with the Drude relaxation frequency.)

A, the "A parameter" in (1), turns out to be the key quantity if interfaces come into play, and this will be proven by experimentally determined data presented in the following.

The correction term $v_{\mathrm{Fermi}} \cdot A/R$ in (1), which was first introduced in 1969 with $A = 1$ [19], consists of two parts: v_{Fermi}/R is the reciprocal time of free flight through the particle of collision-active electrons (i.e. electrons with energies close to E_{Fermi}), while A characterizes the mechanism and the effectivity of a charge transfer process in the interface region.

Only in 1984 it became clear from the pioneering experiments on MPP bandwidths by the Schulze group [20] that the A parameter depends on the chemical composition of the partial surroundings.

Later, Persson and Zaremba [21, 22] developed a theoretical model for A in the jellium approximation. They introduced, instead,

$$\Gamma(R) \approx \Gamma_0 + A^*/R \quad \text{with}$$
$$A^* \approx A \cdot v_{\mathrm{Fermi}} \cdot \left(2\omega_p^2/\omega_s^3\right)/(d\varepsilon_1/d\omega). \tag{3}$$

While A is dimensionless, A^* carries a dimension, e.g. with the unit [eV nm]. Equation (3) is approximative, since, in contrast to A of (1), which is directly connected to the electron dynamics, A^* is a direct measure of Γ, which, as mentioned above, depends on the "dielectric shift" in real materials. We assume the A parameter to be better suited than the MPP bandwidth Γ to characterize dynamic charge transfer processes. We evaluated the A parameter numerically either from (1) or by an explicit fit of Mie's theory to our absorption spectra measured from minute Ag particles in various embedding media.

Pinchuk extended Persson's jellium-based model by taking the single-electron interband excitations into account [9, 23, 24]. His results for the case of silver point to a marked increase of the MPP damping, compared to Persson's data.

Recently, experimental data of the A^* parameter were determined for deposited and embedded Ag and Au particles by Hubenthal et al. [8, 14, 15].

4 Static and dynamic charge transfer

If the free, uncontaminated surface of a metallic nano is transferred into an interface by depositing adatoms as described before, first, a multitude of novel electronic states ("adsorbate states"), localized in the interface, may occur which can—e.g. via the tunneling effect—be occupied by metal electrons from the metal particle. The formation of electronic interface states is qualitatively demonstrated for a single adatom in several publications (e.g. [5, 25]), so we disclaim details here.

Two different charge transfer processes, modeled as "static" and "dynamic interface charge transfer", were presented in 1993 [12], together with their experimental verification.

According to these models, the interface states have two different effects on the MPPs:

4.1 The static charge transfer

Each adatom from the surrounding medium may be bound at the particle surface by physi- or chemisorption at different stable positions on edges, corners or surface planes of the surface. So, the adatom levels of a densely covered surface have, in general, broad energy spectra. If among them there are some low-lying, empty states, they can be permanently occupied by electrons, tunneling from the metallic particle. This "static charge transfer" helps to equilibrate the chemical potential in the new {particle + adsorbate} system. In addition to the "dielectric shift" mentioned above, it induces a frequency shift $\Delta\omega_{\mathrm{Maximum}}$ of the MPPs towards the red, since a certain number of former conduction electrons of the particle, δn, now are bound and localized in the interface layer. These electrons no longer act as metal electrons and contribute no longer to the MPPs. This leads to the above additional red shift, since the frequency positions of MPPs depend on the "free" electron density n. It appears unclear to what extent the thus created electric double layer may supplementarily contribute to the optical extinction spectrum.

Basically, this model describing the story of single adsorbates also applies qualitatively to deposited and to embedded particles, but now we deal with large numbers of adsorbates in thick layers in more or less dense packings at structurally and energetically different parts of the surface. They will interact among each other, thus further increasing the width of their energy level spectrum and the probability for static charge transfer, and causing measurable MPP shifts. The problem of this model is that these states in the strongly inhomogeneous interface layer can rather be predicted up to now. Vice versa, however, their number δn can be determined from the measured peak shift. To measure the latter, the peak position for the clean, free surface must also be known, and this puts high demands on the experiments, since supplementary free particle beam experiments are required. We expect that theoretical interpretations of δn may help to better understanding of interfaces in general and, thus, can support surface science of realistic surfaces/interfaces.

Restricting to very small nanoparticles (i.e. to the "quasistatic approximation" of Mie's theory [3]), the resulting MPP red shift is quantified as [5, 26, 27]

$$\Delta\omega_{\mathrm{Maximum}} \approx -\left\{(n_1)^{1/2} - (n_2)^{1/2}\right\} \cdot \left(e^2/(\varepsilon_0 m_{\mathrm{eff}})\right)^{1/2} \times (2\varepsilon_{\mathrm{Medium}} + \chi_{1,\mathrm{Interband}})^{-1/2}, \tag{4}$$

where n_1 and n_2 are the Drude electron densities in the particle before and after the static charge transfer; e, ε_0 and m_{eff} are elementary charge, electrical field constant and effective mass; $\chi_{1,\mathrm{Interband}}$ is the contribution of interband transitions to the particle susceptibility.

The resulting charging δn in the particle may be high, yet does not induce Coulomb explosion, since, in fact, the static charge transfer merely creates the electric interface double layer of the whole "dressed particle" system, which, as a whole, remains neutral.

The static charge transfer has further important consequences for the particles' properties. Among these are changes of E_{Fermi}, of the surface electron spill-out, of the effective mass, of the optical interband transitions and, possibly, changes of atomic distances and lattice and surface structures. Hence, chemically *novel* nanomaterial can be created. However, the more correct view is to attribute the effect to the whole complex system of particle, interface and surrounding matter.

To give an example: we embedded 2.5-nm Ag particles into a solid C_{60} matrix. Due to static charge transfer these particles lost $\delta n/n_{\mathrm{bulk}} \approx -20\%$ of their conduction electrons (with an A parameter of 1). This means that, roughly, each C_{60} molecule which *directly* touches the surface of an Ag particle extracts *one* conduction electron from the metal. Obviously, these particles, if regarded separately, can no longer be considered to be of silver but a *novel* metal emerges in the nanoscopic state.

4.2 The dynamic charge transfer

Conduction electron "collisions" in the inside of metalic particle are, in general, inelastic concerning momentum and/or energy, in the sense of the classical collective Drude theory. They cause phase disturbances of the single-electron dynamics and, hence, reduce, step by step, the number of the coherent electrons in a plasma excitation which, thus, stepwise fades away. This model is based upon single-electron effects leading to the relaxation of a collective excitation by increasing disorder. The relaxation of the collective excitation by "dephasing" or "decoherence" processes of its members is very effective and leads, in realistic particles, to MPP lifetimes of only a few femtoseconds.

Now we assume that an empty interface level is situated close to the Fermi level of the particle. A conduction electron with v_{Fermi} hitting the particle interface may then tunnel into this level. This appears to be "normal" interface dynamics. The effect, yet, has drastic consequences, if we pick out a time window where a MPP is excited in the particle. Then, the collective *drift* motion of all conduction electrons (alternatively in the quantum picture: the plasmon polariton) is coupled in phase to the incident electrodynamic field. If then there are empty *interface levels* close to E_{Fermi}, electrons can occupy them. After some "residence time" τ_{Res}, the electron can return from the interface level into the particle. τ_{Res} and the propagation time within the three-dimensional interface region, i.e. the whole "excursion times", are statistically varying quantities [5, 26, 27] and, so, the electrons, returning to the particle, have lost the memory of their previous phase in the plasma excitation; they are out of the phase with the excited MPP and no longer contribute.

This "dynamic charge transfer" follows the $1/R$ law [3]. So, its contribution to *dephasing* in (1) may be described by an extra interface contribution term $A_{\mathrm{interface}}$ in (1) which reflects the chemical and structural properties of the interface. We define $A_{\mathrm{interface}}$ as the additive *interface* contribution to the A parameter of the *size* effect in free particles:

$$A = A_{\mathrm{total}} = A_{\mathrm{size}} + A_{\mathrm{interface}}. \tag{5}$$

If the involved interface levels are close to E_{Fermi}, such a decoherence cycle may be almost elastic. It contributes to the process of MPP dephasing (decoherence) with a statistically independent average relaxation frequency which is added, according to the Matthiessen law, to the relaxation frequency of the interior (often inelastic) Drude-like single-electron "collisions".

This simplifying model consists of a *collective* MPP excitation and its relaxation by dephasing of *single* electrons. The existence of the interface influences both.

Important for the efficiency of this process is, among others, the magnitude of the residence time τ_{Res}.

If τ_{Res} is longer than τ_{MPP}, then, after only one such *dephasing* process the electrons hitting the interface are definitively lost for the whole collective excitation process. As shown in the following experimental examples, this "dynamic charge transfer" can decrease the plasmon phase lifetime drastically and, consequently, Γ and the A parameter in (1) increase. Obviously, the efficiency is larger than in simple "collisions" (i.e. Drude-like scattering events) at the *free* surface.

What is most important, the interface-A depends on the chemical and topological composition of the interface. Measuring Γ and A opens, thus, a route to detailed, material-sensitive interface characterization. The A parameter depends on the topology of the many-adatom adsorption and is different for isolated adsorbates, for deposition on a substrate, for a surrounding shell (e.g. due to surface oxidation) and for an extended embedding medium, respectively.

As a conclusion, the two kinds of charge transfer and the according peak shifts and A parameters may yield rich information about electronic properties of particle/surroundings interfaces, if we are able to model them properly in a quantitative way. This appears to be a promising task.

We model $A = A_{\mathrm{interface}}$ by

$$A_{\mathrm{interface}} = f \cdot \left(\Phi \cdot \rho(E_{\mathrm{Fermi}}) \cdot \phi(\tau_{\mathrm{Res}}) \cdot B\right), \tag{6}$$

where Φ means the relative surface coverage with adsorbate atoms, ρ is the density of *un*occupied interface states close to E_{Fermi} per adatom, and $\phi(\tau_{\mathrm{Res}})$ characterizes the efficiency of the contribution of one electron to the MPP

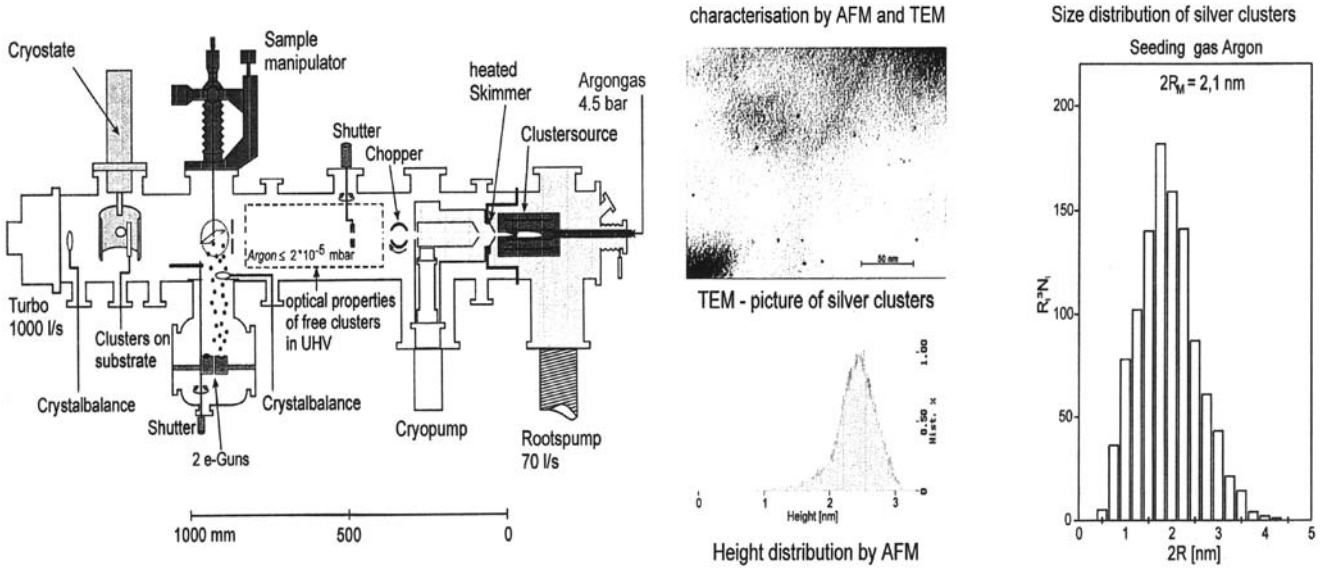

Fig. 3 *Left*: Thermal UHV cluster source THECLA with in situ optical equipment (for details, see [26, 27]). *Center*: TEM micrograph and AFM height histogram of Ag nanos produced by THECLA. *Right*: TEM lateral size histogram of the 2.1-nm Ag particles. Carrier: C foil

dephasing, or, expressed inversely, the average degree of remaining reminiscence of the coherent collective drift phase of the electron, after its return into the particle.

Finally, B is the transfer probability of the energy barrier between particle and interface (if existing), with contributions by the Friedel oscillations and the additional static charge transfer.

5 Own experiments to determine the A parameter

The smaller the particle size, the larger the relative amount of surface atoms and the interface thickness relative to the particle size and, hence, the sensitivity of MPPs to surface/interface effects. The "ideal" experiment would, therefore, be to produce a free beam of solid-state nanos of high quality with very small sizes, which are subsequently embedded in different matrix materials and/or deposited on different substrates, and then to evaluate MPPs and the according A parameters and "free-electron" density changes δn. In a long-term project, this experiment was realized in our groups since 1987, based upon a novel kind of particle source and in situ optical investigation equipment, the thermal cluster source apparatus THECLA (Fig. 3, left). It is described in detail in [26, 27]. Here, we only mention two of the outstanding parameters: the Ag vapor pressure in the source amounts up to 0.5 bar and the seeding gas pressure up to 3 bar. A free-particle beam in the UHV experimental chamber was formed by (partly) adiabatic expansion through a Laval nozzle and additional cooling in cryo-pump equipment. The extreme pressures were necessary to obtain high particle number densities in the free beam (filling factors of $\sim 10^{-11}$), sufficient for direct optical transmission measurements.

Three kinds of optical MPP absorption spectra of the Ag particles were recorded:

- in the free beam, i.e. with clean, uncontaminated free surface,
- after deposition onto arbitrarily chosen solid substrates, which cohere usually evaporated from an e-beam source,
- after embedding into solid surrounding media which were co-deposited with the particles from two e-beam sources.

These experiments were performed with the *same* particles; hence, all differences between the three kinds of spectra are exclusively caused by the different surface/interfaces. Interface effects can, thus, be quantitatively "calibrated" by the results on the free-particle beam.

The particle sizes were selected to exhibit, on the one side, the largest possible nano-effects, and on the other side to be clearly above the molecule/solid-state transition, i.e. a solid-state band structure existed. The THECLA parameters were chosen to produce very small particles from 2 to 4 nm mean diameters with narrow size statistics of less than 30% standard deviation. Different mean sizes were obtained by using different seeding gases ($2R = 2.1$, 3.7, 4.0 nm for Ar, Kr, Xe, respectively). Figure 3 (center and right) shows a size analysis for such Ag nanos by TEM (lateral size) and by AFM (vertical size). The particles were deposited on arc-produced C foil. Within the limits of the respective instrumental accuracies, both, the TEM and AFM diameters coincide, so the particles resemble a spherical shape with only small flat contact areas on the C foil. Existing small influ-

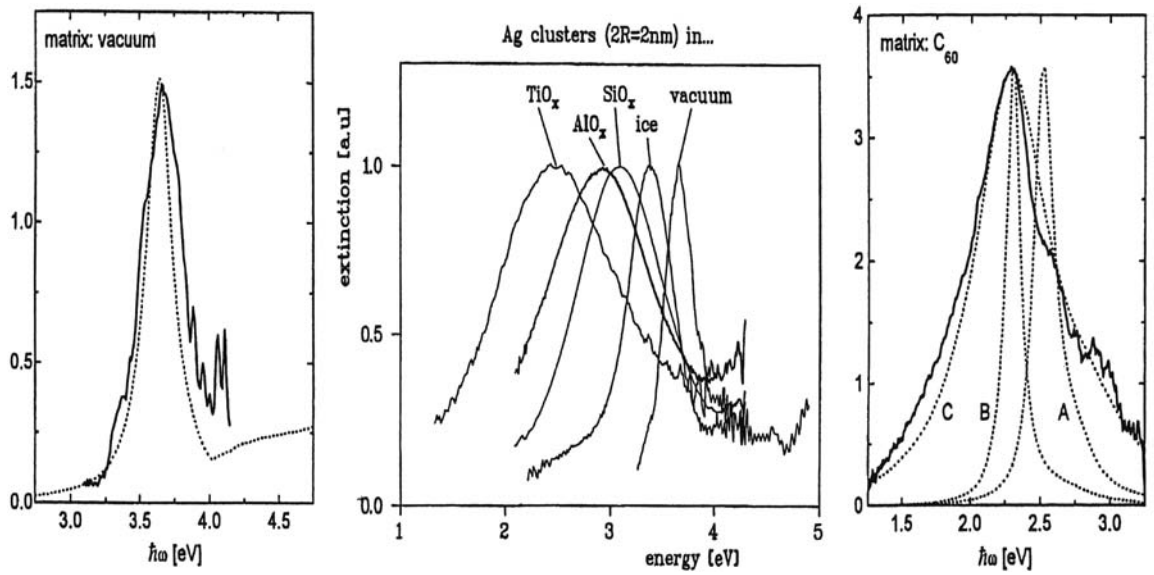

Fig. 4 *Left*: measured absorption spectrum of free Ag nanos ($2R =$ 2 nm) and attempt of simulation by modified Mie theory. *Center*: measured absorption spectra of Ag nanos embedded in various dielectric oxides indicating the "dynamic charge transfer" effect. *Right*: Ag nanos, 2.5 nm, embedded in C_{60}. Demonstration of "static" and "dynamic" charge transfer effects. *Solid curve*: measured absorption spectrum. A: "classical" Mie spectrum. B: spectrum of A corrected for "static" charge transfer. C: spectrum of B but corrected for "dynamic" charge transfer. Optimum fit to the experiment

ences of the size distributions on the optical spectra were numerically controlled by Mie calculations introducing the TEM size histograms. After inspecting possible inhomogeneous broadening effects, we concluded that, in particular, the spectra of the *free* particles are essentially *free from inhomogeneous broadening influences,* after they had been corrected for size distribution. In many-particle systems, additional broadening occurs by electromagnetic particle–particle coupling, according to the generalized Mie theory [3], if next-neighbor distances are below 5 to 10 particle radii. Therefore, we always produced highly diluted many-particle systems (Fig. 3) which are essentially characteristic for the *single* particle. The A parameters and δn values were extracted and "calibrated" with the according free-particle spectrum.

Substantial inhomogeneous broadening, stemming from statistically varying inhomogeneous and/or anisotropic topology of matrix or substrate can, however, not be ruled out for embedded or deposited nanos. They were, however, estimated to be substantially smaller than the observed drastic interface effects themselves.

6 Experimental results: A parameters for free, deposited and embedded nanos

The first and main task in our long-term project was to collect optical extinction spectra of our Ag nanos with systematic variation of the surrounding materials and substrates, while keeping all other Ag particle properties as much unchanged as possible. Resulting A parameters and density changes δn were evaluated applying Mie's theory and dielectric theory; they are considered a first experimental step towards closer knowledge of electronic structures of metal/dielectric interfaces. Due to the lack of better criteria, the *numerical* correspondence of a simulated Mie spectrum with the according measured one was used as indication of the optimum fit.

In Fig. 4 three selected sets of measured absorption spectra are summarized [26–28]: Fig. 4 (left) concerns Ag particles in the free beam and shows attempts to simulate their spectra, Fig. 4 (center) shows spectra of the particles embedded in different oxide matrices and Fig. 4 (right) presents details of the charge transfer investigations especially for embedding in solid C_{60} [29, 30].

In Table 2, A parameter values are presented, derived for about 20 different non-metallic immersion media and, in addition, for five different substrates. All were evaluated to obtain a broad basis for further theoretical interface analyses. Table 2 also includes data of Schulze's group on solidified gases [20].

Only two examples of the according dephasing relaxation times are given in Table 2: for very small and very large A, respectively.

The extrapolation to (fictitious) larger particles of $2R =$ 15 nm (where intrinsic size-effect damping in the particles is only small) was performed with the modified Mie theory.

In the present brief and summarizing article, we now pick out only a few important details about interface prop-

Table 2 *A* parameters of Ag nanos in contact with various media (see e.g. [5]). Data: *theory*: Persson and Zaremba [21, 22]. *Experiments*: *solidified gases*: Schulze and co-workers [20]. *Other solid media*: Kreibig's group [3, 26, 27, 31]. Papers, theses, diploma works (1994–1999) of Cüppers, Fröba, Gartz, Hilger, Hövel, Maaß, Nusch, Pidun, Relitzki, Sonntag, Tenfelde. For details see [3, 26, 27]

Matrix material	Theory	Experiment	Mie plasmon lifetimes
Free clusters	0.29	0.25	7 fs ($2R = 2$ nm) 15 fs (extrapolated to $2R = 15$ nm)
Solid Ne	0.29	0.25	
Ar		0.3	
O_2	0.6	0.5	
CO_2	1.1	0.9	
Na–Si–O glass	1.0	1.0	
Ice		0.5	
Li $F_{(x)}$ ($x \approx 1$)		0.72	
$CaF_{(2-x)}$ ($x \ll 1$)		0.76	
$MgF_{(2-x)}$ ($x \ll 1$)		0.80	
Fullerite (C_{60})		1.0	
$SiO_{(2-x)}$ ($x \ll 1$)		1.3	
ITO		1.5	
$SrTiO_x$		1.5	
$Al_2O_{(3-x)}$ ($x \ll 1$)		1.7	
$TiO_{(2-x)}$ ($x \ll 1$)		1.8	
$P(C_6H_5)_3$		2.0	
SbO_x		2.0	
Si (+ O impurities)		≈3.0	0.6 fs ($2R = 2$ nm)
CrO_x		≈3.0	
Substrates			
$MgF_{(2-x)}$ ($x \ll 1$)		0.55	
ITO		0.57	
SiO_2 (110 K)		0.55	
SiO_2 (300 K)		0.59	
CrO_x		0.59	

Table 3 Contact areas and *A* parameters for Ag particles deposited on different dielectric substrates (Tenfelde, see in [26, 27])

Substrate	MgF_x ($x \approx 2$)	SiO_x ($x \approx 2$)	Cr_xO_y ($x \approx 2$, $y \approx 3$)
Dielectric constant $\varepsilon_{\text{Medium}}$	1.85	2.3	$4.5 + 0.2i$ (at 2.35 eV)
Contact area (interface)	15%	9.5%	<3%
A parameter (deposition)	0.55	0.59	0.59
A parameter (embedding)	0.83	1.3	3.0

erties and interface effects (more information is given in [26, 27]):

(1) The shifts $\Delta\omega_{\text{Maximum}}$ are small compared to the "dielectric shifts" while the dramatic increases in width can surpass, with *A* parameters larger than 1, all observed size effects. The shifts could only be determined with sufficient accuracy by "calibrating" the MPP positions with the free-particle spectra.

(2) Dielectric *oxide* matrices, in general, cause larger broadening than *fluorides*. This means, probably, that the density of empty interface states $\rho(E_{\text{Fermi}})$ in (6) is essentially larger for oxides than for fluorides.

(3) Effects of chemisorbed organic surroundings prove to be of comparable size. Data of $(C_6H_5)_3P$, triphenylphosphine, which is applied as stabilizer for the famous *Schmid clusters* (see e.g. [3]), are: $A = 0.7$ (deposition) and $A \approx 2$ (embedding), respectively. The according shifts amount to $\hbar\Delta\omega_{\text{Resonance}} = 0.03$ and 0.1 eV. In these experiments, the samples were produced by ex situ spin coating from liquid solution.

(4) The surprisingly small experimental value of $A = 0.25$–0.30 of the *free* particles follows the trend of Persson's theory for jellium particles ($A = 0.29$ [21, 22]) and is essentially smaller than expected from the classical "free-path effect" ($A \sim 1$) [3].

(5) The according *dephasing times*, two examples of which are given in Table 2, decrease from $\tau = 15$ fs down to values of $\tau \sim 1$ fs for different matrix materials. In the latter case, the collective excitations are limited to a few oscillation periods only. Hence, it makes little sense to persist in strict conditions of theoretical equilibrium models.

Figure 5 shows that there is a distinct relation between static and dynamic charge transfer: small/large shifts correspond to small/large broadening, and these effects occur in dielectric media with low/high optical polarizabilities (i.e. low/high $\varepsilon_{\text{Medium}}$). In our model this is not very surprising, since both effects are due to the same electronic interface states.

7 A short excursion to deposited nanoparticles

A comparison of Tables 2 and 3 demonstrates, for the examples MgF_2, SiO_2 and Cr_2O_3, that particle *deposition* onto films of these materials with strongly differing $\varepsilon_{\text{Medium}}$ (which were e-beam evaporated on quartz or sapphire slides) only causes *A* parameters slightly varying between 0.55 and 0.59, in drastic contrast to particles embedded in the same materials.

We propose a simplified explanation for this effect: the essential difference between both kinds of samples is that the coverage Φ of (6) is always complete ($\Phi = 1$) in embedding systems, but restricted to the direct contact area in

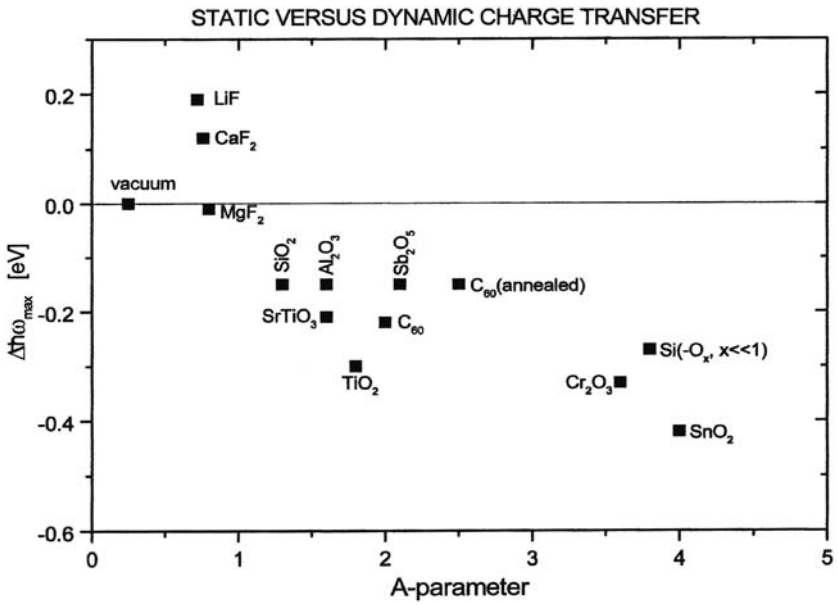

Fig. 5 Summary of investigated optical absorption properties of embedded 2-nm Ag particles: Plot of the peak shifts due to "static" charge transfer against the A parameter due to "dynamic" charge transfer

deposition systems. The coverage Φ, i.e. the contact area, is variable by surface tension induced particle deformations.

By combining the models of Bedeaux and Vlieger and the theory of Yamaguchi (for details see [26, 27]), Tenfelde estimated mean contact areas from optical spectra under varying angles of incidence and polarizations. He found the resulting area to vary for different substrate materials from 15% (MgF_x) down to 3% (Cr_xO_y) of the whole particle surface.

From these results we conclude that the contact area (hence, the mean adatom coverage in (6)) is smaller in systems of high values of $\varepsilon_{\text{Substrate}}$, i.e. high substrate polarizability, while A is larger. This has the consequence that the effects of A (and of ρ, ϕ and B in (6)) are (partly) compensated by the changes of Φ.

Additional experiments with the system of Ag particles on a SiO_2 surface revealed that the contact area changes with temperature, lower ones yielding smaller contact areas and smaller particle deformations (for details see [26, 27]).

Acknowledgements The author and his crew of scientific collaborators are indebted to the DFG, to the Humboldt Foundation and to the EU for financial support in the frame of numerous research projects.

References

1. G. Mie, Ann. Phys. **25**, 377 (1908)
2. U. Kreibig, P. Zacharias, Z. Phys. **231**, 128 (1970)
3. U. Kreibig, M. Vollmer, *Optical Properties of Metal Clusters*. Springer Ser. Mater. Sci., vol. 25 (Springer, Berlin, 1995)
4. A.N. Lebedev, M. Gartz, U. Kreibig, Eur. Phys. J. D **6**, 365 (1999)
5. U. Kreibig, Optics of nanosized metals, in *Handbook of Optical Properties*, vol. II, ed. by R. Hummel, P. Wißmann (CRC Press, Boca Raton, 1997)
6. A. Hilger, Th. von Hofe, U. Kreibig, Nova Acta Leopold. **92**(340), 9 (2005)
7. M. Aeschlimann, Electron dynamics in metallic nanoparticles, in *Encyclopedia of Nanoscience and Nanotechnology*, ed. by H. Nalwa (American Scientific Publishers, Los Angeles, 2004)
8. F. Hubenthal, Dämpfung der lokalisierten Oberflächenplasmon-Polariton-Resonanz, Habilitation thesis, University of Kassel, 2007
9. A.O. Pinchuk, G.C. Schatz, A. Reinholdt, U. Kreibig, Nanotechnol. Res. J. **1**, 1 (2007)
10. V. Schneider, A. Reinholdt, U. Kreibig, T. Weirich, G. Güntherodt, B. Beschoten, A. Tillmanns, H. Krenn, K. Rumpf, P. Granitzer, Z. Phys. Chem. **220**, 173 (2006)
11. T. Klar, M. Perner, S. Grosse, G. von Plessen, W. Spirkl, J. Feldmann, Phys. Rev. Lett. **80**, 42149 (1998)
12. H. Hövel, S. Fritz, A. Hilger, U. Kreibig, M. Vollmer, Phys. Rev. B **48**, 18178 (1993)
13. F. Stietz, J. Bosbach, T. Wenzel, T. Vartanyan, A. Goldmann, F. Traeger, Phys. Rev. Lett. **84**, 5644 (2000)
14. T. Ziegler, C. Hendrich, F. Hubenthal, T. Vartanyan, F. Traeger, Chem. Phys. Lett. **386**, 319 (2004)
15. C. Hendrich, J. Bosbach, F. Stietz, F. Hubenthal, T. Vartanyan, F. Traeger, Appl. Phys. B **76**, 869 (2003)
16. B. Lamprecht, A. Leitner, F.R. Aussenegg, Appl. Phys. B **68**, 419 (1999)
17. J.H. Klein-Wiele, P. Simon, H.G. Rubahn, Phys. Rev. Lett. **80**, 45 (1998)
18. B. Lamprecht, J.R. Krenn, A. Leitner, F.R. Aussenegg, Phys. Rev. Lett. **83**, 4421 (1999)
19. U. Kreibig, C.v. Fragstein, Z. Phys. **224**, 307 (1969)
20. K.P. Charlé, F. Frank, W. Schulze, Ber. Bunsenges. Phys. Chem. **88**, 350 (1984)
21. E. Zaremba, B.N. Persson, Phys. Rev. B **35**, 596 (1987)
22. B. Persson, Surf. Sci. **281**, 153 (1993)
23. A. Pinchuk, G. von Plessen, U. Kreibig, J. Phys. D: Appl. Phys. **37**, 3133 (2004)
24. A. Pinchuk, U. Kreibig, New J. Phys. **5**, 151 (2003)
25. R.W. Gurney, Phys. Rev. **15**, 479 (1935)
26. A. Hilger, Grenzflächenanalyse durch Mie-Plasmon-Spektroskopie an Edelmetallclustern, Thesis, RWTH Aachen, 2001 [www.bth.rwth-aachen.de/edos/ediss.html]

27. M. Gartz, Clusterphysik mit LUCAS, einer neuartigen Laser-Nanoteilchen-Quelle höchster Leistung, Thesis, RWTH Aachen, 2001
28. U. Kreibig, M. Gartz, A. Hilger, H. Hövel, Optical investigations of surfaces and interfaces of metal clusters, in *Advances in Metal and Semiconductor Clusters*, vol. IV, ed. by M. Duncan (JAI Press, London, 1998), pp. 345–393
29. U. Kreibig, A. Hilger, M. Gartz, Ber. Bunsenges. Phys. Chem. **101**, 1593 (1997)
30. U. Kreibig, M. Gartz, A. Hilger, R. Neuendorf, Nanostruct. Mater. **11**, 1335 (1999)
31. U. Kreibig, M. Gartz, A. Hilger, H. Hövel, in *Fine Particle Science and Technology: From Micro- to Nanoparticles*, ed. by E. Pelizetti (Kluwer, Dordrecht, 1996)